atmosphere

Article

Analysis and Research on the Differences in Observed Data of Sand–Dust Weather between China and Mongolia

Yuan You [1], Linchang An [1,*], Siteng Li [2], Bihui Zhang [1] and Jianzhong Zhang [1]

[1] National Meteorological Centre of China Meteorological Administration, Beijing 100081, China; 2008xiaowanzi2008@163.com (Y.Y.)
[2] Institute of Urban Meteorology, Beijing 100089, China
* Correspondence: anlch@cma.gov.cn

Abstract: The difference in meteorological factors (such as weather phenomena, wind speed, and visibility) of sand–dust weather between China and Mongolia from 2011 to 2021 was analyzed using meteorological observational data and international exchange of meteorological observation data. Additionally, consistency analysis was performed by integrating satellite retrieval products with meteorological observation data. The results showed that the average annual frequency of sand–dust weather in Mongolia was significantly higher than that in China. In China, the sand–dust weather was mainly characterized by floating dust or blowing dust, while in Mongolia, it was primarily characterized by blowing dust or a sand and dust storm. The average annual wind speed and visibility during sand–dust weather in Mongolia were relatively higher than those in China. Based on the dust grade standard of China, when the floating dust occurred in Mongolia, there were cases with wind speed > level 3 and visibility > 10 km; when the blowing dust or sand and dust storm occurred in Mongolia, there were cases with wind speed $\leq$ level 3 and visibility > 10 km. In China, the sand–dust weather mainly occurred in the spring, while the sand-dust weather occurred frequently throughout the year in Mongolia. The number of days with dust lasting for 2 days or more in Mongolia exceeded that of China, and Mongolia had a significant impact on the sand–dust weather in China. According to the ground observation data and satellite retrieve products during the dust events, all dust events that significantly affected China and Mongolia during the same period from 2021 to 2022 were classified into three categories; among them, the proportion of types of large-scale sand–dust weather phenomena observed by both satellite and ground observation stations was significantly higher (6 times). By integrating ground observation data and satellite retrieval products and following the dust grade standard of China, the consistent correction of sand–dust weather phenomena was carried out. This laid the foundation for the future development of international dust grade standards and provided technological support for improved dust forecasting services in the Asian region.

Keywords: sand–dust weather; difference; consistency analysis; integrate

check for updates

Citation: You, Y.; An, L.; Li, S.; Zhang, B.; Zhang, J. Analysis and Research on the Differences in Observed Data of Sand–Dust Weather between China and Mongolia. *Atmosphere* **2023**, *14*, 1401. https://doi.org/10.3390/atmos14091401

Academic Editor: Dimitris Kaskaoutis

Received: 4 August 2023
Revised: 26 August 2023
Accepted: 29 August 2023
Published: 5 September 2023

1. Introduction

Sand–dust weather had the characteristics of sudden, strong, and great damage and had caused serious adverse effects on the atmospheric environment. The aerosol particles produced by it have become an important influencing factor in global climate change [1–5]. Northern China, as one of the prone areas for sand–dust weather in Central Asia, frequently experienced disastrous sand–dust weather events. According to statistics, in the past five years, sand–dust weather events in China have occurred more than 10 times on average [6]. The border area between China and Mongolia was one of the main sources of sand–dust weather, and spring was the peak period for sand–dust weather occurrences [7]. Sand–dust weather was influenced by factors such as underlying surface conditions and meteorological conditions, and the greater the surface wind speed, the higher the probability of its occurrence [8]. Similarly, studies have also provided evidence that the occurrence of intense dust weather was influenced by enhanced radiative forcing [9–11]. Sand–dust weather not only affected the atmospheric environment of the source area but also had varying degrees of impact on the upstream and downstream areas along the way [12–15]. Mongolia serves as an upstream source region for dust weather in China [16,17], and the occurrence of disastrous sand–dust weather in Mongolia directly affected the northwestern, northern, and southern regions of China and even impacted South Korea and Japan in the downstream region of China [18]. With the frequent occurrence of sand–dust weather in Mongolia, issues related to monitoring, movement paths, sand formation, sedimentation, forecasting, and early warning systems of dust events in Mongolia have become hot topics and challenges in research [19]. The monitoring methods for sand–dust weather mainly included ground observation and satellite monitoring. Due to limitations in manpower, financial resources, and other factors, ground monitoring often resulted in monitoring information that was single-layer and single-point, which made it difficult to achieve large-scale coverage [20]. Meteorological satellites, with their high resolution and wide spatial coverage, could rapidly acquire dynamic information about dust, and the monitoring results could achieve a relatively high level of accuracy. In addition, multiple satellite retrieval products have been formed based on dust identification, such as aerosol optical depth (AOD) and infrared difference dust index (IDDI), among others.

In recent years, domestic and international scholars have carried out a series of research studies on sand–dust weather between China and Mongolia. Zhang et al. [21] conducted a statistical analysis of dust events from 2000 to 2002 and found that 70% of the sand–dust weather in China originated from Mongolia. Zhang et al. [22] conducted an analysis of 12 severe dust events using observational data and NCEP reanalysis data, and the results showed that the movement paths of severe sand and dust storms in China could be classified into three categories: Westward, northwestward, and southern Xinjiang basin. Among them, both the westward and northwestward paths of the sand–dust weather originated in Mongolia. An et al. [23] summarized the relationship between surface conditions and climate change by statistically analyzing the spatial-temporal distribution of dust events from 2007 to 2016. Chen et al. [24] found that a comprehensive understanding of the sources of dust in China and Mongolia was crucial for revealing the mechanisms of dust generation, dust forecasting, desertification control, and other related aspects. Duan et al. [25] tested the monitoring effectiveness of the Infrared Difference Dust Index (IDDI) from the FengYun meteorological satellite and found that the dust index had good monitoring effectiveness.

Currently, research on sand–dust weather in China and Mongolia mainly focuses on short-term or specific dust events, and there is a lack of long-term studies on the characteristics of sand–dust weather over time. Moreover, due to inconsistent observation standards for sand–dust weather phenomena in the ground observation data exchanged internationally, the records of sand–dust weather were chaotic, which greatly affected the statistical analysis and forecasting of sand–dust weather. In order to conduct a more comprehensive and accurate study of the characteristics of sand–dust weather in China and Mongolia, this paper conducted a study on the characteristics of sand–dust weather in China and Mongolia from 2011 to 2021, as well as their correlation with wind speed and visibility. It summarized the differences in sand–dust weather phenomena between China and Mongolia and the impact of Mongolia on sand–dust weather in China. Additionally, by integrating the observed station data and satellite inversion products (IDDI) during the dust events from 2021 to 2022, a consistent correction of sand–dust weather phenomena was carried out. The above research has preliminary developed a dust level correction method suitable for East Asia, which laid the foundation for the future development of international dust grade standards and providing technological support for improved dust forecasting services in the Asian region.

2. Materials and Methods

The ground observation data (weather phenomena, visibility, wind speed) of China and Mongolia were obtained from the ground observation stations of the China Meteorological Administration and the international exchange of meteorological observation stations of the World Meteorological Organization, spanning the 10-year period from 2011 to 2021. Sand–dust weather in China mainly occurred in the northern region north of about 35° N [26]. Therefore, the spatial domain was 75°~130° E, 30°~55° N. This study conducted analysis and research on sand–dust weather based on the data from 125 ground observation stations in China and 66 international exchange meteorological observation stations in Mongolia. According to the analysis of the transport paths of dust, the paths were divided into westward paths and northwestern paths. Ejinaqi Station of China and Gubantes Station of Mongolia, which were closest in straight-line distance, were selected as representative stations for western Inner Mongolia of China and western Mongolia, respectively. Erlianhot Station of China and Zamyn Uud Station of Mongolia, which were closest in straight-line distance, were selected as representative stations for central Inner Mongolia of China and central Mongolia, respectively (Figure 1). The geographical location of the relevant stations is shown in Figure 1.

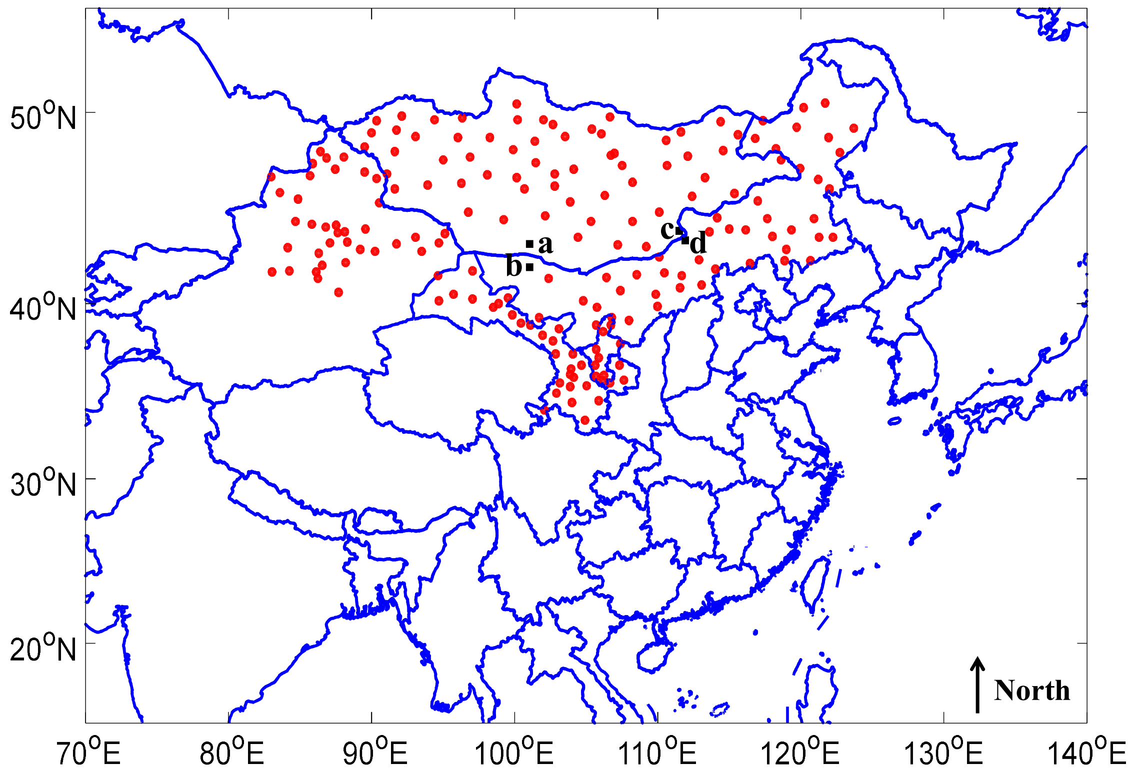

Figure 1. Distribution of observation sites a (Gubantes station of Mongolia), b (Ejinaqi station of China), c (Zamyn Uud station of Mongolia), d (Erlianhot station of China).

The infrared difference dust index (IDDI) was defined as the difference between the real-time target brightness temperature monitored by satellite and the background surface brightness temperature [27]. Its value represented the infrared temperature attenuation caused by dust [28,29]. As an indicator of dust concentration in the atmosphere, the IDDI had a close positive relationship with the distribution of dust; the higher the value, the more dust there was. The monitoring results showed that the IDDI could accurately monitor dust events in real time [25]. The satellite data used in this study were obtained from the FengYun-4A meteorological satellite (FY-4A) [30], and the IDDI provided by it was compared and fused with the ground observation data.

3. Results and Discussion

3.1. Spatial Distribution Differences of Ground Observation Data between China and Mongolia

3.1.1. The Spatial Distribution of Dust Frequency

The China Meteorological Administration (CMA) graded the weather phenomenon of sand–dust weather into five levels: Floating dust; blowing dust; sand and dust storms (SDS); severe SDS; and super-severe SDS [23]. Due to the limited number of observation samples above the level of severe SDS, this study statistically analyzed the observation samples of SDS, severe SDS, and super-severe SDS together, collectively referred to as SDS. Figure 2 shows the annual average frequency of sand–dust weather at different levels from 2011 to 2021. Among them, the solid circles represented annual average frequencies greater than 0, while the hollow circles represented annual average frequencies equal to 0, the proportion of stations referred to the ratio of the number of dust stations to the total number of stations, and the frequency proportion referred to the ratio of the frequency of dust at each level to the total frequency of dust. As shown in Figure 2a, there was a significant difference in the average annual frequency of dust between China and Mongolia; the average annual frequency of sand–dust weather in Mongolia was noticeably higher than that in China. Among them, In Mongolia, the proportion of stations with an average annual frequency of dust exceeding 10 times was 77%, while in China, the proportion is only 26%. China was mainly characterized by floating dust and blowing dust, with the frequency proportions of floating dust and blowing dust being 31% and 64%, respectively. Mongolia was primarily characterized by blowing dust and SDS, with the frequency proportions of blowing dust and SDS being 35% and 58%, respectively.

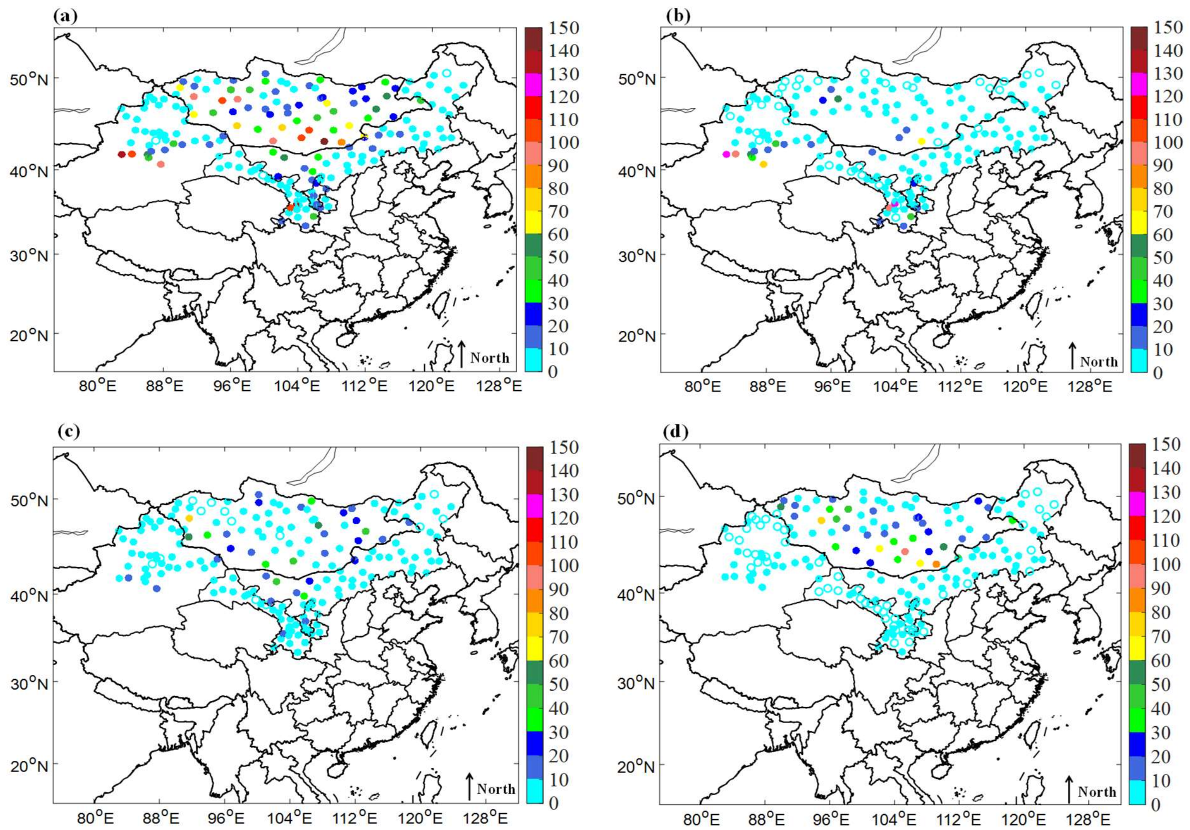

Figure 2. The spatial distribution of average annual frequencies of (**a**) dust, (**b**) floating dust, (**c**) blowing dust, (**d**) SDS between China and Mongolia.

3.1.2. Distribution of Wind Speed

The occurrence of sand–dust weather required sufficient wind speed, which provided a crucial driving mechanism for the generation and transportation of sand–dust weather [31].

The dust grade standard [32] defined wind speed ≤ level 3 (5.4 m/s) as floating dust and wind speed > level 3 (5.4 m/s) as blowing dust or SDS. As shown in Figure 3a, the annual average wind speed of sand–dust weather in Mongolia was generally higher than that in China; the proportion of stations with wind speeds greater than level 3 in Mongolia and China was 95% and 69%, respectively. In China, the wind speeds during sand–dust weather were consistent with the dust grade standards; however, in Mongolia, during floating dust weather, there were 21 stations with an annual average wind speed greater than level 3 (Figure 3b); during blowing dust weather, there were 11 stations with an annual average wind speed ≤ level 3 (Figure 3c); and during SDS weather, there was one station with a wind speed ≤ level 3 (Figure 3d).

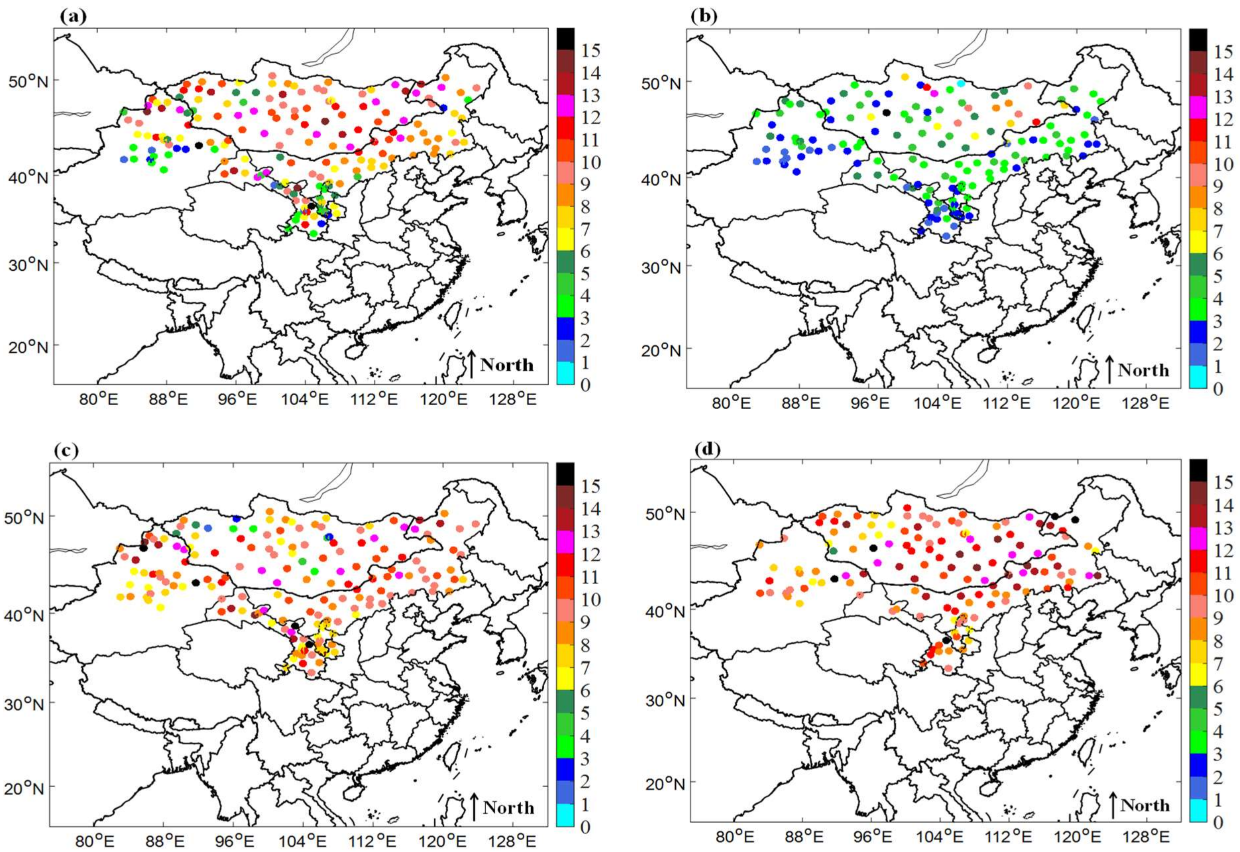

Figure 3. Spatial distribution of average annual wind speed of (**a**) dust, (**b**) floating dust, (**c**) blowing dust, (**d**) SDS in China and Mongolia.

3.1.3. Distribution of Visibility

Visibility, as an important indicator for the classification of dust intensity grade, was the major factor contributing to the hazards of sand–dust weather [33]. The dust grade standards defined visibility of less than 10 km as floating dust, visibility ranging from 1 to 10 km as blowing dust, and visibility less than 1 km as SDS. In order to explore the differences in visibility between China and Mongolia, the annual average visibility corresponding to each level of sand–dust weather was analyzed. As shown in Figure 4a, the annual average visibility during sand–dust weather in China was consistently less than 10 km, while in Mongolia, the annual average visibility during sand–dust weather at various stations was significantly higher than that in China. The visibility during sand–dust weather in China was consistent with the dust grade standards; however, when Mongolia experienced floating dust, blowing dust, and SDS, there were 35 stations, 53 stations, and 59 stations with annual average visibility exceeding 10 km, respectively.

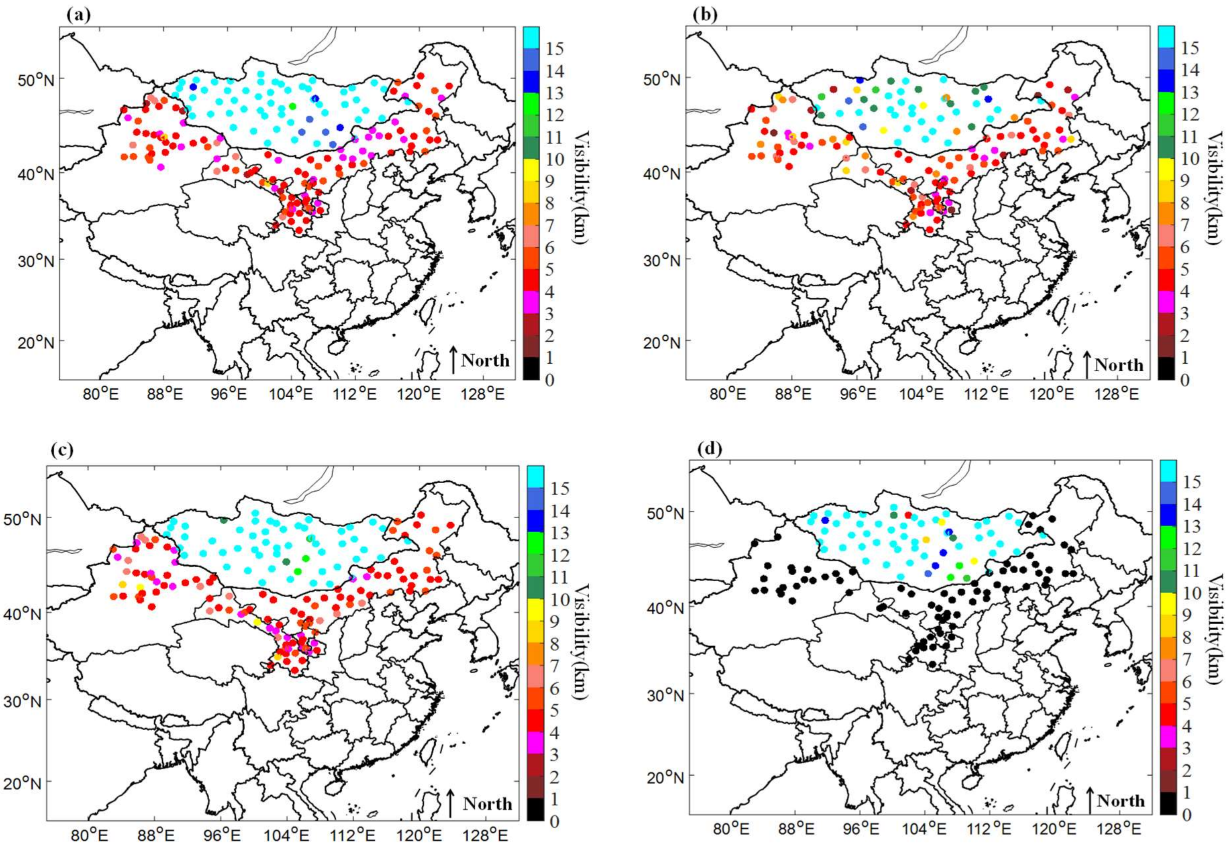

Figure 4. Spatial distribution of average annual visibility of (**a**) dust, (**b**) floating dust, (**c**) blowing dust, (**d**) SDS in China and Mongolia.

Based on the statistical results regarding the annual average frequency, annual average wind speed, and annual average visibility of sand–dust weather between China and Mongolia, it could be observed that Mongolia and China had different criteria for determining sand–dust weather phenomena. Does this inconsistent observation standard affect the forecast of sand–dust weather? Based on the above issues, this study focused on conducting long-term analysis and research on the observation data in the key border area between China and Mongolia.

3.2. Long-Time Temporal Distribution of Ground Observation Data

3.2.1. Annual Distribution of Dust Frequency

Annual statistics were conducted on the frequency of sand–dust weather at four representative sites: Ejinaqi Station (representing the western part of Inner Mongolia, China), Gubantes Station (representing the western part of Mongolia), Erlianhot Station (representing the central part of Inner Mongolia, China), and Zamyn-Uud Station (representing the central part of Mongolia) from 2011 to 2021.

As shown in Figure 5a, the annual frequency of dust in western Mongolia was relatively high year by year from 2011 to 2021, especially in 2013, 2014, and 2021, where the frequency reached 138, 132, and 150 times, respectively. However, except for 2019 (64 times), the frequency of dust in western Inner Mongolia of China remained below 60 times. As shown in Figure 5e, except for 2015, the frequency of dust in central Mongolia was generally higher than that in central Inner Mongolia of China; especially in 2012 and 2016, the frequency of dust in central Mongolia reached 122 and 111 times, respectively, while except for 2015 (63 times) and 2016 (84 times), the frequency in central Inner Mongolia of China remained below 60 times.

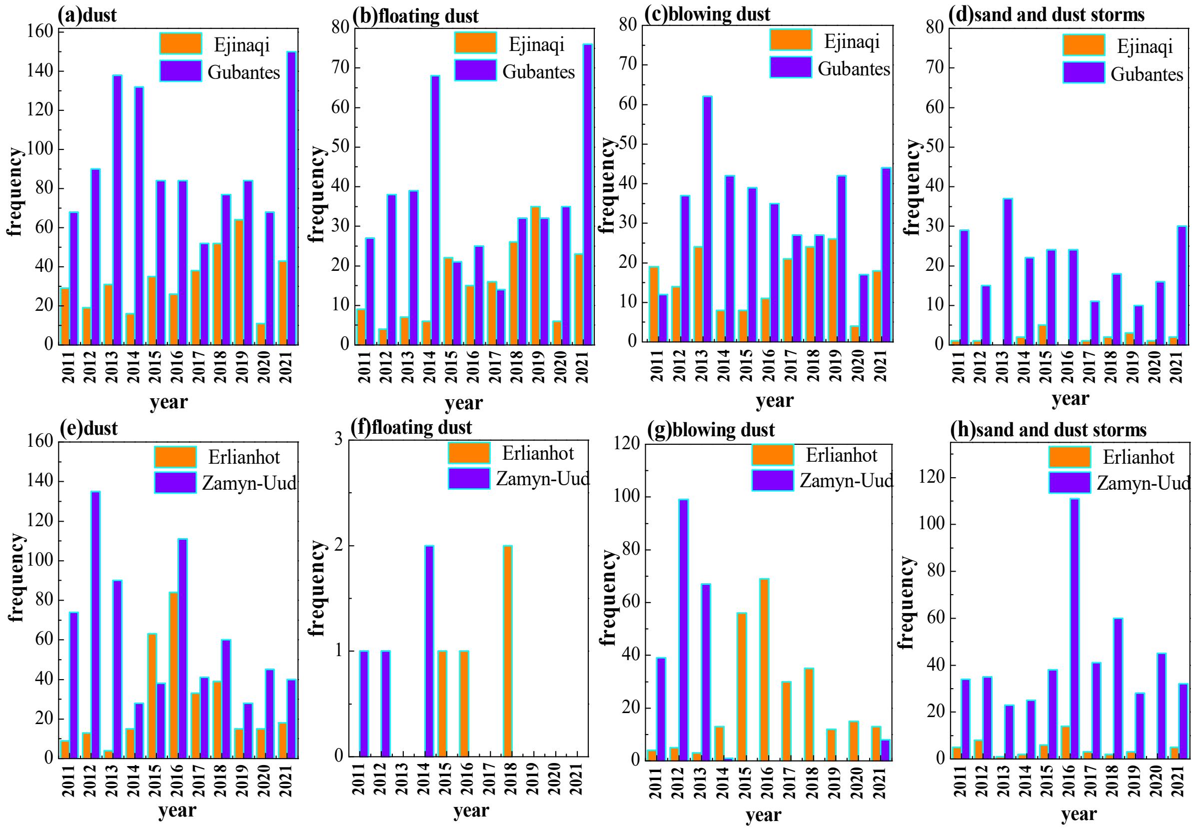

Figure 5. The interannual variation of (**a**) dust, (**b**) floating dust, (**c**) blowing dust, (**d**) SDS frequency in western Inner Mongolia, China, and western Mongolia. The interannual variation of (**e**) dust, (**f**) floating dust, (**g**) blowing dust, (**h**) SDS frequency in central Inner Mongolia, China, and central Mongolia.

The frequency of SDS in western Mongolia from 2011 to 2021 was significantly higher year by year compared to western Inner Mongolia, China (Figure 5d). However, the frequency of floating dust (Figure 5b) and blowing dust (Figure 5c) in western Inner Mongolia of China was relatively high, with the sum of the annual frequency of floating dust and blowing dust accounting for more than 85%, while the annual frequency ratio of SDS was less than or equal to 10%. The annual frequency of SDS in central Mongolia from 2011 to 2021 was significantly higher than that in central Inner Mongolia of China, especially from 2014 to 2021, where the annual frequency ratio accounted for more than 80% year by year. Meanwhile, the frequency of blowing dust in central Inner Mongolia of China was relatively high year by year, especially from 2013 to 2021, where the frequency ratio accounted for over 70% year by year.

3.2.2. The Probability Density Distribution of Different Wind Speeds during Dust Weather

For further research, the probability density distribution of wind speed frequency during sand–dust weather at four representative stations from 2011 to 2021 was separately analyzed according to different intervals (every 1 m/s interval). The selected data met the condition that the frequency was greater than 0. The probability of different wind speed intervals was represented by Va, the frequency of each wind speed interval was represented by n, and the total frequency of wind speeds was represented by N. Therefore, Va = n/N × 100%. The average probability of wind speeds (Vave) was defined as the ratio of the sum of the probabilities of each wind speed to the number of wind speed intervals. After calculation, when sand–dust weather occurred in western Inner Mongolia of China (Figure 6a), the wind speeds with Va $\geq$ Vave ranged from 3 to 8 m/s; among them, wind speeds of floating dust were all $\leq$ level 3, and wind speeds with Va $\geq$ Vave ranged from 3 to 5 m/s. Wind speeds were all > level 3 during blowing dust and SDS; among them, wind speeds with Va $\geq$ Vave ranged from 6 to 8 m/s during blowing dust, and wind speeds with Va $\geq$ Vave ranged from 7 to 9 m/s during SDS. When sand–dust weather occurred in western Mongolia (Figure 6b), the wind speeds with Va $\geq$ Vave ranged from 10 to 16 m/s. Compared with western Inner Mongolia of China, the probability of wind speeds surpassing level 3 was 42.5% during floating dust, and wind speeds with Va $\geq$ Vave ranged from 2 to 8 m/s. When blowing dust and SDS occurred, the proportion of frequency with wind speeds $\leq$ level 3 accounted for 1.1% and 0.4%, respectively. Among them, wind speeds with Va $\geq$ Vave ranged from 10 to 16 m/s during blowing dust, and wind speeds with Va $\geq$ Vave ranged from 11 to 16 m/s during SDS.

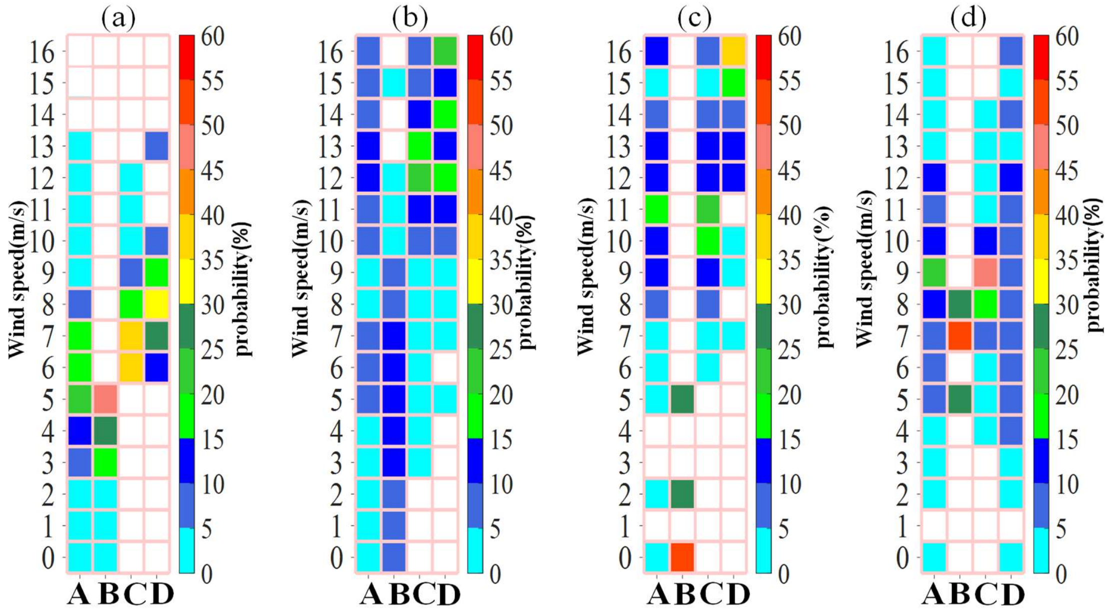

Figure 6. The probability distribution of frequency in the interval of wind speed (**a**) in western Inner Mongolia, China (**b**) in western Mongolia (**c**) in central Inner Mongolia, China (**d**) in central Mongolia. **A**. Dust; **B**. Floating dust; **C**. Blowing dust; **D**. SDS.

As shown in Figure 6c, when sand–dust weather occurred, the wind speeds with Va $\geq$ Vave were all $\geq$ 9 m/s in central Inner Mongolia of China. Among them, when floating dust occurred, wind speeds were all $\leq$ level 3, with only 4 occurrences; when blowing dust and SDS occurred, wind speeds were > level 3, and wind speeds with Va $\geq$ Vave ranged from 9 to 13 m/s during blowing dust, and wind speeds with Va $\geq$ Vave ranged from 12 to 16 m/s during SDS. Compared with central Inner Mongolia of China, where wind speeds with Va $\geq$ Vave ranged from 5 to 12 m/s in central Mongolia (Figure 6d), there were only 4 occurrences of floating dust weather in the central part of Mongolia, with 3 occurrences of wind speeds greater than level 3. When blowing dust occurred, the probability of wind speeds $\leq$ level 3 accounted for 1.9% and 16.9%, respectively. Among them, wind speeds with Va $\geq$ Vave ranged from 8 to 10 m/s during blowing dust, and wind speeds with Va $\geq$ Vave ranged from 5 to 12 m/s, 14 m/s, and 16 m/s during SDS.

3.2.3. The Probability Density Distribution of Different Visibility during Sand–Dust Weather

The probability density distribution of different visibility during sand–dust weather between China and Mongolia was analyzed, and the visibility frequency of sand–dust weather at four representative stations from 2011 to 2021 was statistically counted according to different intervals. The selected data all met the criterion of a frequency greater than 0. As shown in Figure 7, the probability of different visibility intervals was represented by Visa, the visibility frequency of each interval was represented by nvis, and the total visibility frequency was represented by Nvis. Therefore, Visa = $\frac{\mathrm{nvis}}{\mathrm{Nvis}} \times 100\%$. The average probability of visibility was defined as (Visave), which is the ratio of the sum of visibility probabilities to the number of visibility intervals in sand–dust weather. After calculation, when sand–dust weather occurred in western Inner Mongolia of China (Figure 7a), the visibility with Visa ≥ Visave ranged from 3 to 10 km, the visibility of floating dust was all ≤ 10 km, among which the visibility with Visa ≥ Visave ranged from 3 to 10 km, the visibility of blowing dust ranged from 1 to 10 km, and with the visibility of Visa ≥ Visave ranging from 3 to 10 km, the visibility of SDS was all less than 1 km. However, in the western region of Mongolia, the visibility of sand–dust weather was consistently greater than 10 km (Figure 7b), and the probability of visibility less than 1 km was 0 during SDS.

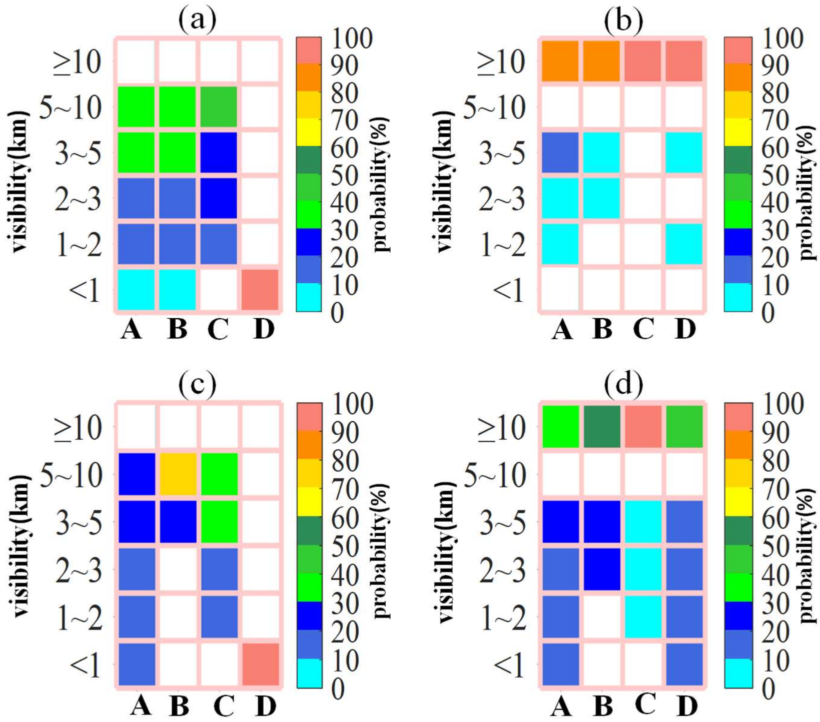

Figure 7. The probability distribution of visibility frequency (**a**) in western Inner Mongolia, China, (**b**) in western Mongolia, (**c**) in central Inner Mongolia, China, (**d**) in central Mongolia. **A**. Dust; **B**. Floating dust; **C**. Blowing dust; **D**. SDS.

When sand–dust weather occurred in central Inner Mongolia of China (Figure 7c), the visibility with Visa ≥ Visave ranged from 3 to 10 km, the visibility of floating dust was all ≤ 10 km, with only 4 occurrences, the visibility of blowing dust ranged from 1 to 10 km, with the visibility of Visa ≥ Visave ranging from 3 to 10 km, and the visibility of SDS was all less than 1 km. Compared with the central Inner Mongolia of China, the visibility of SDS was consistently greater than 10 km (Figure 7d).

3.2.4. Comparison of Occurrence Time of Sand–Dust Weather at Stations near the China-Mongolia Border

The intensity and duration of sand–dust weather in Mongolia had a significant impact on China. The above research conclusion indicated that Mongolia experienced a higher frequency of SDS compared to China. In order to study the impact of Mongolia's sand–dust weather on China, this study selected the years 2013 and 2016, which had the highest frequency of SDS in western and central Mongolia, respectively. According to the specific dates of sand–dust weather occurrence, as shown in Figure 8, in China, sand–dust weather mainly occurred in the spring, while in Mongolia, sand–dust weather occurred frequently throughout the year. Based on the definition by Chen Yi et al. [20], the occurrence of sand–dust weather (including floating dust, blowing dust, and SDS) at a particular observation station was defined as the number of dust days. According to statistics, the number of dust days in western Inner Mongolia of China was 19 days, while in western Mongolia, it was 62 days. The number of consecutive dust days lasting for 2 days or more in western Mongolia (14 times) exceeded that of western Inner Mongolia of China (3 times). The number of dust days in central Inner Mongolia was 42 days, and the number of dust days in central Mongolia was 59 days. The number of consecutive dust days lasting for 2 days or more in central Mongolia (16 times) exceeded that of central Inner Mongolia of China (12 times).

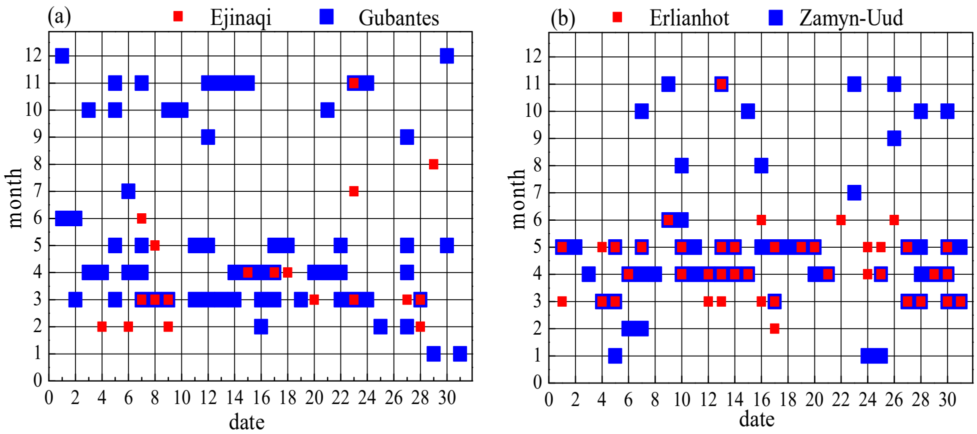

Figure 8. Distribution of start time of dust occurrence in (**a**) 2013 and (**b**) 2016.

In terms of specific occurrence time, Mongolia had a significant impact on sand–dust weather in China. As shown in the figure, in western Inner Mongolia of China, the start time of sand–dust weather occurrences lagged behind or coincided with Mongolia, and the proportion of dust days accounted for 73.7%. Similarly, in central Inner Mongolia of China, the start time of sand–dust weather occurrences lagged behind or coincided with Mongolia, with the proportion of dust days accounting for 85.7%. Therefore, it could be seen that Mongolia had a significant impact on sand–dust weather in China, with central Mongolia having a more pronounced influence on the central Inner Mongolia of China. This was likely due to the fact that the representative stations in central Inner Mongolia of China were closer to central Mongolia. When influenced by strong winds, the upstream dust was quickly transported to central Inner Mongolia of China, resulting in more frequent sand–dust weather in that region.

3.3. Comparative Analysis and Consistent Integration of Ground and Satellite Observation Data on Dust Events between Mongolia and China

3.3.1. Statistical Analysis of Ground and Satellite Observation Data

The meteorological satellite played a crucial role in detecting and tracking the occurrence, development, and distribution of sand–dust weather [34]. In this study, all the dust events that affected both Mongolia and China from 2021 to 2022 were selected, and the selected dust events met the following criteria: Large-scale dust weather phenomena were observed at ground observation stations in Mongolia and China, and satellite observation images were not obscured. A comparative analysis of ground and satellite observation data was conducted for these events. The statistical results are shown in Table 1, and the dust events were divided into three categories: Type A represented cases where the satellite observed extensive dust in Mongolia but there was no corresponding real-time sand–dust weather observed phenomena on the ground. Type B represented cases where both satellite and ground observations simultaneously detected widespread sand–dust weather. Type C indicated cases where extensive sand–dust weather phenomena were observed on the ground in Mongolia, but there was no corresponding real-time observation of sand–dust weather from satellites.

Table 1. The statistical analysis of ground observation data and satellite data on dust events in China and Mongolia.

Type Classification	Comparative Time	Locations of Dust of the Same Level Both China and Mongolia from Satellite Retrieval Products		The Corresponding Level of Dust on Ground Observation	
		China	Mongolia	China	Mongolia
Type A	16 March 2021	Central Inner Mongolia	Southeast Mongolia	Floating dust	None
Type B	27 March 2021	Central Inner Mongolia	Southeast Mongolia	Blowing dust	SDS
Type B	15 April 2021	Western Inner Mongolia	Southern Mongolia	Blowing dust	SDS
Type B	26 April 2021	Central and western Inner Mongolia	Southern Mongolia	Blowing dust	SDS
Type B	6 May 2021	Western Inner Mongolia	Southern Mongolia	SDS	SDS
Type C	3 March 2022	Western Inner Mongolia	None	Blowing dust occurred in western Inner Mongolia	Blowing dust occurred in central and southern Mongolia, while SDS occurred in the southern region
Type B	20 April 2022	Western Inner Mongolia	Southern Mongolia	Blowing dust	SDS
Type B	25 April 2022	Western Inner Mongolia	Central Mongolia	Blowing dust	SDS
Type C	5 May 2022	Western Inner Mongolia	None	Blowing dust occurred in western Inner Mongolia	Floating dust, blowing dust, and SDS occurred in the southern region of Mongolia

Nine strong dust events from 2021 and 2022 were selected for comparative analysis at typical time points. Among them, the proportion of type B dust events was significantly higher (6 times), followed by type C (2 times), and type A had only one occurrence. Except for the dust event on 6 May 2021, the dust events of type B showed consistent dust levels between the satellite inversion products in both China and Mongolia; moreover, the satellite-retrieved dust locations were consistent with the ground-based observations; however, there were differences in the intensity of dust levels between the satellite retrievals and ground-based observations. In most cases, the ground-based observations of dust levels corresponding to the same dust level retrieved by satellite were mostly floating dust or blowing dust in China, while they were SDS in Mongolia. This conclusion was consistent with the previous finding that floating dust or blowing dust was predominant in China, whereas Mongolia experienced a much higher frequency of SDS.

3.3.2. Consistency Fusion of Ground and Satellite Data

Two typical dust events were selected, type A (16 March 2021) and type B (20 April 2022), to compare and analyze ground observation data and satellite retrieval products between Mongolia and China, and according to the dust grade standard of China, the sand–dust weather phenomenon was consistently corrected. As shown in Figure 9a, In the ground-based observation data, there was no sand–dust weather phenomenon in Mongolia (Figure 9a), while large areas of sand–dust weather were observed in the central and southern regions of Mongolia through satellite retrieval products (Figure 9b). By combining the ground-based observation data with the satellite retrieval products, we added ground-based observation data that corresponds to the satellite-retrieved dust locations, and according to the dust grade standard of China, the intensity of the added dust was consistently adjusted (Figure 9c). As shown in Figure 9d, large areas of sand–dust weather had been observed in the vicinity of the China–Mongolia border. The satellite-retrieved dust products (IDDI) in southern Mongolia and central Inner Mongolia of China showed the same level (Figure 9e), and the dust positions retrieved from the satellite and the dust positions observed on the ground were consistent, but there was a difference in the intensity of the dust levels between the ground-based observations. In southern Mongolia, the ground-based observation indicated SDS, while in central Inner Mongolia of China, it indicated blowing dust. Therefore, combining the satellite-retrieved products and ground-based observations, and following dust grade standards, the SDS in southern Mongolia was adjusted to blowing dust (Figure 9f).

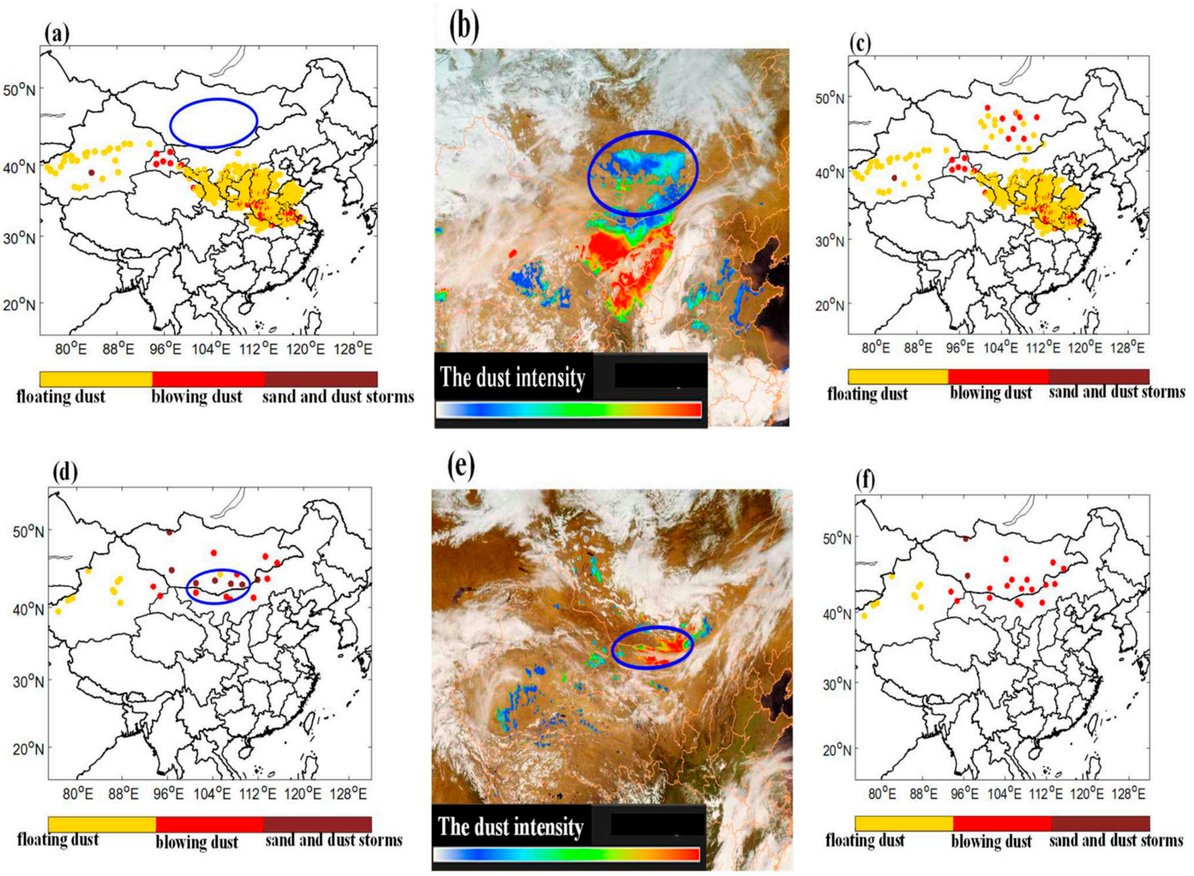

Figure 9. Comparison of ground and satellite observations during the strong dust events. (**a**) The ground observation at 14:00 on 16 March 2021. (**b**) The satellite observation at 14:00 on 16 March 2021. (**c**) The fusion data of ground and satellite observation at 14:00 on 16 March 2021. (**d**) The ground observation at 14:00 on 20 April 2022 (**e**). The satellite observation at 14:00 on 20 April 2022. (**f**) The fusion data of ground and satellite observation at 14:00 on 20 April 2022. The blue circle is the calibrated area.

4. Conclusions

As a kind of catastrophic weather, sand–dust weather had serious adverse effects on the atmospheric environment and human health. The difference in meteorological factors (such as weather phenomena, wind speed, and visibility) of sand–dust weather between China and Mongolia from 2011 to 2021 was analyzed. Additionally, consistency fusion was carried out between satellite inversion products (IDDI) and meteorological observation data. The following conclusions could be drawn from the results obtained in this study:

1. The average annual frequency of sand–dust weather in Mongolia was noticeably higher than in China. China is mainly characterized by floating dust and blowing dust, while Mongolia is primarily characterized by blowing dust and SDS. The annual average wind speed and visibility during sand–dust weather in Mongolia was generally higher than in China; when floating dust occurred, there were cases with a wind speed > level 3 and a visibility > 10 km, while when blowing dust and SDS occurred, there were cases with a wind speed $\leq$ level 3 and a visibility > 10 km.
2. The frequency of dust in western Mongolia from 2011 to 2021 was significantly higher year by year compared to China, especially the frequency of SDS, which was much higher than that in China. When sand–dust weather occurred in western Inner Mongolia of China and western Mongolia, the wind speeds with Va $\geq$ Vave ranged from 3 to 8 m/s and 10 to 16 m/s, respectively. The visibility with Visa $\geq$ Visave ranged from 3 to 10 km and above 10 km, respectively. When sand–dust weather

occurred in central Inner Mongolia of China and central Mongolia, the wind speeds with Va $\geq$ Vave ranged from 6 to 12 m/s and above 9 m/s, respectively, and the visibility with Visa $\geq$ Visave ranged from 3 to 10 km and above 10 km, respectively. The number of consecutive dust days lasting for 2 days or more in Mongolia exceeded that of China.

3. Comparing the ground observation data and satellite retrieval products of dust events, the dust events were classified into three types: The proportion of type B was significantly higher (6 times), followed by type C (2 times), and type A had only one occurrence. By integrating ground observation data and satellite retrieval products, and following the dust grade standard of China, the consistent correction of dust weather phenomena was carried out.

Author Contributions: Conceptualization, Y.Y. and L.A.; methodology, Y.Y., L.A. and S.L.; validation, L.A., B.Z. and J.Z.; formal analysis, Y.Y.; investigation, Y.Y., L.A. and S.L.; writing—original draft preparation, Y.Y.; writing—review and editing, L.A. and S.L.; visualization, Y.Y., L.A. and B.Z.; supervision, S.L. and J.Z.; project administration, Y.Y. and L.A.; funding acquisition, L.A. and B.Z. All authors have read and agreed to the published version of the manuscript.

Funding: This research was co-funded by the Joint Fund of the National Natural Science Foundation of China and the China Meteorological Administration (Grant No. U2242209), National Natural Science Foundation of China (41905121), The Open Project of the Key Laboratory of Atmospheric Chemistry, China Meteorological Administration (2022B01).

Informed Consent Statement: Informed consent was obtained from all subjects involved in the study.

Conflicts of Interest: The authors declare no conflict of interest.

References

1. Pye, K. *Aeolian Dust and Dust Deposits*; Academic Press Inc. Ltd.: London, UK, 1987; pp. 113–126.
2. Middleton, N. Desert dust hazards: A global review. *Aeolian Res.* **2017**, *24*, 53–63. [CrossRef]
3. Chan, Y.; McTainsh, G.; Leys, J.; McGowan, H.; Tews, E. Influence of the 23 October 2002 dust storm on the air quality of four Australian cities. *Water Air Soil Pollut.* **2005**, *164*, 329–348. [CrossRef]
4. Leys, J.; Heidenreich, S.; Strong, C.; McTainsh, G.; Quigley, S. PM10 concentrations and mass transport during "Red Dawn"—Sydney 23 September 2009. *Aeolian Res.* **2011**, *3*, 327–342. [CrossRef]
5. Raupach, M.; McTainsh, G.; Leys, J. Estimates of dust mass in recent major dust storms. *Aust. J. Soil Water Conserv.* **1994**, *7*, 20–24.
6. An, L.C.; Nan, Y.; Zhang, B.H. *Dust Weather Almanac*; China Meteorological Press: Beijing, China, 2021.
7. Liu, J.T.; Zheng, M.Q. Climatic Characteristics of Strong and Very Strong Sandstorms in the Middle and West Parts of Inner Mongolia. *Plateau Meteorol.* **2003**, *22*, 51–64.
8. Kurosaki, Y.; Mikami, M. Recent frequent dust events and their relation to surface wind in East Asia. *Geophys. Res. Lett.* **2003**, *30*, 14. [CrossRef]
9. Chen, Y.; Chen, S.Y.; Zhou, J.; Zhao, D.; Bi, H.R.; Zhang, Y.; Alam, K.; Yu, H.P.; Yang, Y.X.; Chen, J.Y. A super dust storm enhanced by radiative feedback. *NPJ Clim. Atmos. Sci.* **2023**, *6*, 90. [CrossRef]
10. Gui, K.; Yao, W.R.; Che, H.Z.; An, L.C.; Zheng, Y.; Li, L.; Zhao, H.J.; Zhang, L.; Zhong, J.T.; Wang, Y.Q.; et al. Record-breaking dust loading during two mega dust storm events over northern China in March 2021: Aerosol optical and radiative properties and meteorological drivers. *Atmos. Chem. Phys.* **2022**, *12*, 7905–7932. [CrossRef]
11. Yao, W.R.; Gui, K.; Wang, Y.Q.; Che, H.Z.; Zhang, X.Y. Identifying the dominant local factors of 2000–2019 changes in dust loading over East Asia. *Sci. Total Environ.* **2021**, *777*, 146064. [CrossRef]
12. Nguyen, H.; Riley, M.; Leys, J.; Salter, D. Dust Storm Event of February 2019 in Central and East Coast of Australia and Evidence of Long-Range Transport to New Zealand and Antarctica. *Atmosphere* **2019**, *10*, 653. [CrossRef]
13. Aili, A.; Xu, H.L.; Kasim, T.; Kasim, T.; Abulikemu, A. Origin and transport pathway of dust storm and its contribution to particulate air pollution in northeast edge of Taklimakan Desert, China. *Atmosphere* **2021**, *12*, 113. [CrossRef]
14. Gui, K.; Yao, W.; Che, H.; An, L.C.; Zheng, Y.; Li, L.; Zhao, H.; Zhang, L.; Zhong, J.T.; Wang, Y.Q.; et al. Two mega sand and dust storm events over northern China in March 2021: Transport processes, historical ranking and meteorological drivers. *Atmos. Chem. Phys. Discuss* **2021**, *1*, 36.
15. Kavan, J.; Láska, K.; Nawrot, A.; Wawrzyniak, T. High Latitude Dust Transport Altitude Pattern Revealed from Deposition on Snow, Svalbard. *Atmosphere* **2020**, *11*, 1318. [CrossRef]

16. Chen, S.Y.; Zhao, D.; Huang, J.P.; He, J.Q.; Chen, Y.; Chen, J.Y.; Bi, H.R.; Lou, G.T.; Du, S.K.; Zhang, Y.; et al. Mongolia Contributed More than 42% of the Dust Concentrations in Northern China in March and April 2023. *Adv. Atmos. Sci.* **2023**, *40*, 1549–1557. [CrossRef]
17. Gui, K.; Che, H.Z.; Yao, W.R.; Zheng, Y.; Li, L.; An, L.C.; Wang, H.; Wang, Y.Q.; Wang, Z.L.; Ren, H.L.; et al. Quantifying the contribution of local drivers to observed weakening of spring dust storm frequency over northern China (1982–2017). *Sci. Total Environ.* **2023**, *894*, 164923. [CrossRef]
18. An, L.C.; Zhang, H.D.; Gui, H.L.; Zhang, T.H. Analysis of a Sand and Dust Weather Process Affecting North China and Huanghuai in Spring 2015. *Meteorol. Mon.* **2018**, *44*, 180–188.
19. Shao, Y.; Dong, C.H. A review on East Asian dust storm climate modeling and monitoring. *Glob. Planet. Change* **2006**, *52*, 1–22. [CrossRef]
20. Zhang, P.; Zhang, X.Y.; Hu, X.Q.; Qi, J.; Dong, C.H. Satellite remote sensing and analysis of a dust event in 2006. *Clim. Environ. Res.* **2007**, *12*, 302–308.
21. Zhang, K.; Gao, H.W.; Zhang, R.J.; Zhu, Y.J.; Wang, Y.S. Sources and movement routes of sand-dust aero sols and their impact probabilities on china seas in 2000–2002. *Adv. Earth Sci.* **2005**, *20*, 627–636.
22. Zhang, G.Y.; Zhao, S.X.; Sun, J.H. Analysis of Climatological Characteristics of Severe Dust Storms in Recent Years in the Northern China. *Clim. Environ. Res.* **2004**, *9*, 101–115.
23. An, L.C.; Che, H.Z.; Xue, M.; Zhang, T.H.; Wang, H.; Wang, Y.Q.; Zhou, C.H.; Zhao, H.J.; Gui, K.; Zheng, Y.; et al. Temporal and spatial variations in sand and dust storm events in East Asia from 2007 to 2016: Relationships with surface conditions and climate change. *Sci. Total Environ.* **2018**, *633*, 452–462. [CrossRef] [PubMed]
24. Chen, J.; Li, G.J. Geochemical studies on the source region of Asian dust. *Sci. China (Earth Sci.)* **2011**, *41*, 1279–1301. [CrossRef]
25. Duan, H.; Guo, N.; Huo, W.; Qin, H.; Ma, Y. The Comparison of the Prediction Efficiency of GRAPES-SDM Dust-Storm Model and the Satellite Remote Sensing Monitoring. *J. Desert Res.* **2014**, *34*, 1617–1623.
26. Chen, Y.; Shang, K.Z.; Wang, S.G.; Li, Y. Characteristics of sand-dust weather in northern china from 2002 to 2010 and its relationship with surface wind speed and NDVI. *J. Desert Res.* **2012**, *32*, 1702–1709.
27. Cao, G.Z.; Zhang, P.; Chen, L.; Zheng, Z.J.; Hu, X.Q. Duststorm detection by merging meteorological visibility with remote sensing IDDI. *Remote Sens. Technol. Appl.* **2013**, *28*, 588–593.
28. Ackerman, S.A. Remote Sensing Aerosols Using Satellite Infrared Observations. *J. Geophys. Res.* **1997**, *102*, 17069–17079. [CrossRef]
29. Wald, A.; Kaufman, Y.J.; Tanre, D.; Gao, B.-C. Daytime and Nighttime Detection of Mineral Dust over Desert Using Infrared Spectral Contrast. *J. Geophys. Res.* **1998**, *103*, 32307–32313. [CrossRef]
30. Yang, J.; Zhang, Z.Q.; Wei, C.Y.; Lu, F.; Guo, Q. Introducing the new generation of Chinese geostationary weather satellites, Feng Yun-4(FY-4). *Bull. Am. Meteorol. Soc.* **2016**, *98*, 1637–1658. [CrossRef]
31. Zhang, Z.C.; Pan, K.J.; Zhang, Y.; Han, L.Y. Sand transport characteristics above gobi surface during a dust storm in northern China. *J. Desert Res.* **2023**, *43*, 130–138.
32. *GB/T 20480-2017*; Classification of Sand and Dust Weather. China National Standardization Administration Committee: Beijing, China, 2017.
33. Li, X.; Hu, X.Q.; Cui, C.X.; Li, J. Research on Dust Aerosol Optical Properties in South Tarim Basin and Classification of Different Dusty Weather in China. *J. Desert Res.* **2005**, *25*, 488–495.
34. Liu, D.; Zhang, W.; Chen, Y.; Yan, J.L. Analysis of the Mechanism and Transmission of Dust in Northwest China Based on Satellite Remote-sensing Data. *J. Desert Res.* **2014**, *34*, 1605–1616.